



Published in final edited form as:

Mater Sci Eng C Mater Biol Appl. 2018 December 01; 93: 61–69. doi:10.1016/j.msec.2018.07.061.

Vascular extracellular matrix and fibroblasts-coculture directed differentiation of human mesenchymal stem cells toward smooth muscle-like cells for vascular tissue engineering

Na Li^{a,b}, Hanna Sanyour^{a,b}, Tyler Remund^c, Patrick Kelly^{c,d}, Zhongkui Hong^{a,b,*}

^aDepartment of Biomedical Engineering, University of South Dakota, SD, United States of America

^bBioSNTR, Sioux Falls, SD, United States of America

^cSanford Health, Sioux Falls, SD, United States of America

^dSchool of Medicine, University of South Dakota, SD, United States of America

Abstract

Construction of an artificial vascular graft is widely considered a promising strategy in vascular tissue engineering. However, limited sources of functional vascular smooth muscle cells (VSMCs) remain a major obstacle in vascular tissue engineering. In this study, we innovatively developed an approach to obtain functional VSMCs by onsite differentiating human bone marrow-derived mesenchymal stem cells (MSCs) directed by decellularized extracellular matrix (ECM) and fibroblasts. The resulting cells and ECM-cells constructs were characterized by real time RT-PCR, immunofluorescence staining, cell contractile functions, and migration capacity. Our results showed both ECM and fibroblasts induced MSCs differentiation toward VSMC-like cells with increased transcription of marker genes, upregulated expression of contractile apparatus proteins, and enhanced functional activity of VSMC phenotype. Interestingly, our findings revealed that native ECM and fibroblasts-coculture had a higher potential to promote MSCs differentiation into VSMCs than growth factors cocktail (GFC) supplemented culture, thereby providing a potential source of VSMCs for blood vessel constitution.

Keywords

Mesenchymal stem cells; Differentiation; Extracellular matrix; Smooth muscle cells; Fibroblasts; Growth factors cocktail

*Corresponding author at: Biomedical Engineering Department, University of South Dakota, 4800 N Career Ave, Suite 221, Sioux Falls, SD 57107, United States of America. Zhongkui.Hong@usd.edu (Z. Hong).

Conflicts of interest

There are no conflicts of interest to declare.

Appendix A. Supplementary data

Supplementary data to this article can be found online at <https://doi.org/10.1016/j.msec.2018.07.061>.

1. Introduction

Successful constitution of tissue-engineered blood vessels possessing natural structure and functions of native arteries remains a daunting challenge in vascular tissue engineering, in spite of many efforts have been made in this field [1,2]. Vascular cells and biological scaffolds are two essential elements that constitute robust bioartificial vessels [3]. Although various novel biomimetic materials were developed over the past decades [4], limited availability of endothelial cells and smooth muscle cells for vessel constitution persists as a bottleneck problem in vascular tissue engineering [5]. Many efforts have been made on the procurement of endothelial cells [6–8], but the necessity of obtaining functional vascular smooth muscle cells (VSMCs) is largely neglected [3]. Present in the media layer, VSMCs are critical to maintaining the structural and functional integrity of blood vessels by providing physical support and regulating the blood flow and pressure by contracting and relaxing in response to exogenous stimulus [9]. However, the access to autologous VSMCs from biopsies is limited due to their difficulty in acquirement of pure populations, restricted proliferation potentials and rapidly declining cell functions during *in vitro* expansion [3,10]. Therefore, obtaining sufficient functional VSMCs is a prerequisite for developing vessel substitutes in vascular tissue engineering.

To address the challenge in VSMCs source restrictions, smooth muscle-like cells differentiated from embryonic stem cells (ESCs) [11,12], mesenchymal stem cells (MSCs) [13–17], and induced pluripotent stem cells (IPS) [1,18] have gained great attention and exhibited highly promising results. Maturation of VSMCs is a complicated process driven by multiple chemical, physical, and biological cues. Currently, the differentiation of stem cells toward VSMCs is often guided by growth factor stimulation, such as transforming growth factor-beta 1 (TGF β 1), platelet-derived growth factor BB (PDGF-BB) and bone morphogenetic protein-4 (BMP4) on 2D substrates [15,16] and/or 3D synthetic biomaterials [2,10,19,20]. Nevertheless, chemical induction initiated by growth factors might cause unspecialized differentiation [10] or undesirable cell apoptosis [3]. Natural decellularized extracellular matrix (ECM) exhibited excellent biological properties and biocompatibility [21,22], and has been applied in the reconstruction of different tissues, such as ligaments, tendons, and abdominal wall with desired shape and mechanical properties of the tissues from which they were derived [23,24]. More interestingly, cell-matrix and cell-cell interactions have been recognized to play crucial roles in various biological events including cell adhesion, proliferation, migration, and differentiation [25,26]. The microenvironment, both ECM and a number of different types of stromal cells such as fibroblasts surrounding VSMCs, provide many benefits for facilitating the differentiation of stem cells toward VSMCs and their maturation during vessel formation [27].

In this study, we tested our hypothesis that microenvironmental signals (ECM or fibroblasts-coculture) may have the capability to direct stem cell differentiation toward a matured VSMC phenotype similar to the ability of soluble growth factors. We tested the effect of natural decellularized blood vessel ECM scaffold, indirectly cocultured fibroblasts, and growth factor cocktail (GFC) composed of TGF β 1, PDGF-BB and BMP4 on human bone marrow-derived MSCs differentiation toward VSMCs. Human VSMCs were used as the control VSMCs lineage. In addition, a 3D coculture model was developed to evaluate the

combined effect of the three major factors mentioned above on differentiation of MSCs into VSMCs.

2. Materials and methods

2.1. Preparation of decellularized ECM scaffolds

Fresh porcine carotid arteries (Fig. S1a) were kindly provided as gift by Alumend (Sioux Falls, SD). After trimming excess connective tissues and fat, the carotid arteries were washed completely with phosphate buffered saline (PBS), and then decellularized according to the protocol described previously with minor modifications [28]. Briefly, carotid arteries were incubated in 3-[(3-cholamidopropyl) dimethylammonio]-1-propanesulfonate (CHAPS) buffer (8 mM CHAPS, 1 M NaCl, and 25 mM EDTA) for 22 h, followed by brief washes with PBS three times. Next, carotid vessels were treated for 24 h with sodium dodecyl sulfate (SDS) buffer composed of 1.8 mM SDS, 1 M NaCl, and 25 mM EDTA, followed by complete washes with PBS ten times. After that, the carotid vessels were incubated with 0.2 mg/ml DNase and 1 mg/ml RNase in PBS for 16 h at 37 °C, and then washed thoroughly with PBS ten times. Lastly, the decellularized ECM (Fig. S1b) were cut into small discs with 5 mm diameter (Fig. S1c) with tissue punch and stored at -80 °C. All decellularization steps were performed with agitation and under sterile conditions. All reagents were purchased from Sigma Aldrich (Sigma, St. Louis, MO).

2.2. Cell maintenance and differentiation

Human bone marrow-derived MSCs (P₁-P₅, ATCC, Manassas, VA) were maintained in MSC culture medium (ATCC) supplemented with MSC growth kit (ATCC). Human VSMCs (P₁-P₃, ATCC) were grown in VSMC culture medium (ATCC) supplemented with VSMC growth kit (ATCC). Human fibroblasts (P₆-P₁₀, ATCC) were cultured in Dulbecco's modified Eagle's medium (DMEM, Invitrogen) containing 10% fetal bovine serum (FBS, ATLANTA Biologicals, Lawrenceville, GA). All cells were subcultured at about 90% confluency and the culture media was refreshed every 2 days.

To evaluate the effects of decellularized vessel ECM and fibroblasts on the differentiation of MSCs into VSMCs, MSCs were cultured in different conditions as follows: (1) MSCs maintained in complete MSC culture medium were defined as MSC group; (2) MSCs were seeded in the upper side of 12-well Transwell (Cat. No. 3460, Corning) with a final concentration of 3×10^4 cells/well, and 1×10^5 fibroblasts were seeded in the lower side of Transwell. The indirect cocultures of MSCs and fibroblasts were conducted with complete MSC culture medium in the apical compartment and fibroblast culture medium in the basolateral compartment; (3) Decellularized vessel ECM scaffolds were immersed in 70% ethanol for 60 min and followed by washes with PBS 3 times, and then equilibrated at 37 °C for another 48 h in complete MSC medium. The residual medium were removed with sterile gauze before MSCs were seeded into adventitial surface of the scaffolds (6×10^4 cells/scaffold) and grew in complete MSC medium; (4) MSCs cultured in complete MSC medium supplemented with growth factor cocktail (GFC) composed of 10 ng/ml TGFβ1, 25 ng/ml PDGF-BB, and 2.5 ng/ml BMP4 (all from Invitrogen) were defined as GFC group; (5) MSCs cultured in the 3D system (Fig. S1d), which combined all three factors

that examined in this work, *i.e.*, ECM, coculture with fibroblast, and GFC, were defined as combined 3D coculture model group. Briefly, SMCs seeded in ECM scaffolds were placed in the upper chamber of Transwell and cocultured with fibroblasts that were seeded in the lower chamber. The cocultures were carried out with complete MSC medium containing GFC in the apical compartment and fibroblasts medium in the basolateral compartment; (6) VSMCs maintained in VSMC culture medium were set as positive control. All the cells were maintained at 37 °C in a 5% CO₂ humidified incubator, and changed media every other day.

2.3. Histological analysis and scanning electron microscopy (SEM) examination

Fresh carotid arteries, decellularized vessel ECM scaffolds, and the ECM-MSCs reconstituted tissue prepared by seeding MSCs in the ECM scaffold and differentiated in the combined 3D coculture models were fixed with 4% paraformaldehyde (Affymetrix, CA) at 4 °C overnight, followed by washes with PBS three times. The paraffin-embedded sections (5 µm thickness) were prepared by Sanford Research (Sioux Falls, SD) and stained with hematoxylin and eosin dyes (Sigma) or Masson's trichrome dyes (Sigma). Images were acquired using an inverted phase contrast microscopy (IX83, Olympus microscope).

The fresh carotid arteries, decellularized ECM scaffold, and the ECM-MSCs reconstituted tissue in combined 3D coculture models were fixed with 2.5% glutaraldehyde (Sigma) overnight at 4 °C, and dehydrated in a series of ethanol with increasing concentration (25%, 50%, 75%, 95% and 100%) before lyophilization. The dried samples were then mounted onto stubs, sputtered with gold, and visualized with SEM (FEI Quanta 450).

2.4. Cell viability evaluation and F-actin staining

To assess the effect of ECM, fibroblasts, and GFC on MSCs viability, the ECM-MSCs reconstituted tissue in combined 3D coculture model on day 1, 7, and 14 were stained with calcein-AM/EthD-1 solution (Invitrogen) as described in previous publication [29]. Live cells were stained green, whereas dead cells were stained red. The samples were observed under confocal microscopy (IX83 FV1200, Olympus).

To evaluate the effect of ECM, fibroblasts, GFC, and the combined effect of all the three factors on F-actin expression in MSCs, the cells harvested from each experimental condition were visualized by phalloidin-FITC staining. Briefly, the samples were fixed with 4% paraformaldehyde at 4 °C overnight, followed by staining with phalloidin-FITC and Hoechst 33342 (Abcam, Cambridge, MA) for F-actin and nucleus, respectively. The fluorescence images were acquired using confocal microscopy.

2.5. Real-time RT-PCR analysis

To compare the transcript level of VSMC characteristic genes between different experimental groups, total RNA was extracted using TRIzol reagent (Invitrogen) according to the manufacturer's instruction, and quantified by spectrophotometric analysis at 260 nm wavelength. Thereafter, a portion of 200 ng RNA underwent reverse transcription in a 20 µL reaction mixture using High Capacity cDNA Reverse Transcript kit (Applied Biosystems, Forster City, CA). Lastly, a fast Real-Time RT-PCR System (Applied Biosystems 7500)

was employed to conduct real-time PCR with Taqman gene expression assays (Applied Biosystems). The relative gene expression level for α -actin (Hs00426835), calponin (Hs00206044), and smoothelin (Hs00199489) was normalized to β -actin (Hs01060665). Each sample was performed in triplicate.

2.6. Immunofluorescence staining

Immunofluorescence staining was employed to further explore the difference of VSMC marker protein expression levels between different experimental groups. The cells resulted from six experimental groups described above were trypsinized and seeded in 24-well plate (Thermo Fisher Scientific) with cover-slips (Thermo Fisher Scientific). After being cultured overnight, the cells were fixed with 4% paraformaldehyde followed by permeabilization with 0.5% Triton-X-100 solution (Sigma) for 20 min. Subsequently, the samples were blocked with 1% bovine serum albumin (BSA, Sigma) for 20 min, and then incubated with mouse anti-human antibodies (1: 50) including anti- α -actin (Sigma), anti-calponin (Sigma), anti-smoothelin (Abcam), anti-myosin heavy chain (MHC, Sigma), and anti-SM-22 α (Abcam) at 4 °C overnight. After being washed with PBS three times, the samples were incubated with the FITC-conjugated goat anti-mouse IgG (Invitrogen) at 37 °C for 2 h, and then stained with Hoechst 33342 to label cell nuclei. The fluorescence images were acquired with confocal microscopy.

2.7. Functional analysis

Firstly, cell contractility was evaluated by cell area decrease in response to vascular agonists as previously described [1, 30]. The cells resulted from six experimental groups described above were trypsinized and seeded in 24-well plate with a final concentration of 1×10^4 cells/well. After being cultured overnight, the cells were washed with PBS twice followed by stimulating with 50 mM KCl or 1 mM carbachol (Sigma) for 15 min. Images were acquired using a phase contrast microscope (IX83, Olympus), and the decrease in cell area was analyzed using Image J.

Secondly, cell migratory activity toward PDGF-BB gradient, a smooth muscle cell chemoattractant, was measured using 24-well Transwell plate with 8 μ m pore size filters (Cat. No. 3464, Corning). The cells from six experimental groups described above were trypsinized and loaded in the upper chamber with a final concentration of 2.5×10^4 cells/well. Meanwhile, 10 ng/ml PDGF-BB (Invitrogen) in serum-free medium was added in the lower chamber. After incubation at 37 °C for 6 h, migrated cells were fixed with 4% paraformaldehyde followed by staining with Hoechst 33342, and then counted manually in ten random fields per sample.

Lastly, a collagen gel contraction assay was carried out using 2 mg/ml rat tail type I collagen solution (COL1, Corning). Briefly, the cells resulted from six experimental groups described above were harvested and embedded in neutral collagen solution at the density of 1.5×10^5 cells/ml. 100 μ l COL1-cells suspension were added in a 12-well plate (Corning) and allowed for polymerization for 1.5 h at 37 °C. The collagen gels were then dissociated with a spatula and allowed to contract for 24 h. Images were taken using Olympus microscope (DP22), and the areas of contracted gels were measured by Image J.

2.8. Statistical analysis

All reported values were averaged ($n = 3$ except for specific experiments where indications are provided) and expressed as mean \pm standard deviation (SD). Statistical differences were analyzed with two-sample t -test assuming equal variances, and the value of $P < 0.05$ was considered statistically significant.

3. Results

3.1. Characterization of decellularized carotid scaffolds

To determine the decellularization efficiency, histological analysis of both native carotid and decellularized ECM scaffolds were performed and the results were shown in Fig. S2. HE staining clearly showed the complete removal of cellular and nucleic components in the decellularized ECM (Fig. S2b) compared to native carotid (Fig. S2a). In addition, the decellularized vessel ECM appeared to be a loose and multilayered structure. A similar observation was made using Masson's trichrome staining (Fig. S2c and 2d), which also provided evidence for the well-preserved ECM structures predominantly composed of collagen fibers in the arterial walls after decellularization (Fig.S2d). Moreover, SEM observation for the adventitial surface of the carotids was performed for both native and decellularized samples. The adventitia of the decellularized scaffold (Fig. S2f) exhibited a significantly rougher surface than that of native carotid arteries (Fig. S2e). To further test the efficiency of the decellularization process, residual DNA content was analyzed quantitatively for decellularized ECM scaffolds and native carotid arteries. Acellular ECM scaffolds showed an average residual DNA of 0.18 ± 0.05 mg/scaffold (5 mm diameter), which was significantly lower than 6.17 ± 0.30 mg/scaffold that contained in native artery (Fig. S2 g). The significantly reduced remaining DNA content in the decellularized scaffolds was consistent with the histological staining observations.

3.2. Cell viability and morphology assessment for the multi factors-combined 3D coculture model

To identify whether the microenvironment provided by ECM, fibroblasts and GFC is favorable for MSCs growth and differentiation, the cell viability of the combined 3D coculture model was evaluated by live-dead staining after different culture periods. MSCs seeded in the combined 3D model not only exhibited high viability after 1 day (Fig. 1a), but also kept their high viability through 1 week (Fig. 1b) and even for 2 weeks (Fig. 1c), suggesting the microenvironment provided by the combined 3D coculture model which incorporated decellularized ECM, stromal cells and GFC facilitated cell attachment and growth. Furthermore, the adventitial surface of acellular scaffolds recellularized with MSCs was visualized by SEM. After 1 day of cultivation, a loose and discontinuous cell layer was formed on the rough surface of decellularized ECM where some gaps between ECM fibers can be observed (Fig. 1d). After 1 week, the adventitia became denser and smoother (Fig. 1e), and after 2 weeks, the entire surface of the scaffold was homogeneously covered by cells and the matrix proteins newly secreted by the cells (Fig. 1f). Simultaneously, HE staining was applied to study the detailed growth profile of MSCs on the ECM scaffold in the combined 3D coculture model. The results showed the growth depth into the decellularized ECM scaffolds increased progressively as a function of culture time (Fig. 1g, h, i). All these

findings supported the fact that decellularized ECM, stromal cells and GFC are favorable for MSCs growth and proliferation. Additionally, F-actin of cells in the combined 3D coculture model were labeled with phalloidin to visualize the morphological characteristics of MSC-derived VSMC like cells. There was almost no stress fiber in the cell on day 1 (Fig. 1j), indicating weak F-actin expression, but lots of stress fibers were clearly visible on day 7 (Fig. 1k), and further increased after 2 weeks of cultivation (Fig. 1l), suggesting the combined 3D coculture microenvironment model facilitates the differentiation of MSCs into VSMCs.

Furthermore, to compare the separate effect of ECM, fibroblasts, and GFC on F-actin expression, each group of cells was stained by phalloidin, respectively. Consistent with what was observed in combined 3D coculture model staining (Fig. 1k and l), cells from combined 3D coculture model displayed a high F-actin fluorescence intensity (Fig. 2j) similar to native VSMCs (Fig. 2l). More interestingly, similar to the GFC group, cells from both ECM and fibroblast groups (Fig. 2d–2h) demonstrated a higher F-actin fluorescence intensity than MSCs (Fig. 2b), while cells from all six experimental groups appeared to have a spindle-like morphology under phase contrast microscopy (Fig. 2a, c, e, g, i and k). Taken together, both decellularized ECM and fibroblasts have a strong capability for facilitating the differentiation of MSCs toward VSMCs similar to the GFC, which is regularly used as MSCs differentiation inducer.

3.3. Gene and protein expression of VSMC-specific markers in MSCs-derived VSMCs

To further test the potential roles played by ECM and fibroblasts in MSCs differentiation into VSMCs, gene and protein expression levels of various VSMCs-specific marker proteins were examined on cells harvested from the six experimental groups on day 14 using both real time RT-PCR and immunostaining, respectively. As shown in Fig. 3, each marker gene, including α -actin, calponin, and smoothelin was significantly upregulated in each experimental group compared to negative control (MSCs). Strikingly, the transcript level of α -actin in each experimental group was even higher than positive control (VSMCs). Moreover, the expression levels of calponin and smoothelin in combined 3D model exhibited a synergistic effect of ECM, fibroblasts, and GFC. Subsequently, five VSMC-specific contractile proteins (α -actin, calponin, smoothelin, MHC, and SM-22 α) were immunofluorescence-stained for cells harvested from six experimental groups on day 14, respectively, and the representative confocal images were presented in Fig. 4. In consistence with the mRNA expression level assayed by real time RT-PCR, the cells from all four differentiation experimental groups exhibited relative high fluorescence intensity for each VSMCs-specific marker protein compared to negative control (MSCs), and surprisingly, the influence exerted by fibroblasts and ECM appeared to be more evident than that of GFC. Specifically, the expressions of all marker proteins in cells from both fibroblast-coculture and ECM groups were at similar level to native VSMCs. These results provided robust evidence for the hypothesis that decellularized ECM matrix and fibroblasts play a regulatory role in MSCs differentiation toward VSMCs.

3.4. Functional evaluation of the MSCs-derived VSMCs-like cells

To evaluate the inductive effect of ECM, fibroblasts and GFC on the differentiation of MSCs into functional VSMCs, two VSMCs-specific functions including cell contraction and migration were tested for the six groups of cells. As shown in Fig. S3 and Fig. S4, at least 50% of cells in each group appeared to contract in response to vasoconstrictors KCl and carbachol. Negative control MSCs reduced cell area by $16.64\% \pm 2.76\%$ or $16.60\% \pm 2.37\%$ in response to the stimulations with KCl or carbachol (Fig. 5a and b). In contrast, exposure to these agonists induced a significant decrease in cell area for all other groups of cells ($P < 0.05$), except GFC group in response to carbachol ($P > 0.05$).

As presented in Fig. 5c and Fig. S5, VSMC-like cells harvested from the combined 3D coculture model exhibited the highest migratory capacity (3.72 times higher than MSCs migration) toward PDGF-BB gradient, even higher than positive control (VSMCs). Compared to MSCs, the cells from ECM group, fibroblast coculture group and GFC group also demonstrated significantly higher migration activity ($P < 0.001$), indicating the inductive capacity of ECM and fibroblasts are comparable to that of GFC.

Cells-populated collagen lattice contraction assay was performed to further assess the contractibility of MSC-derived VSMCs. All groups of cells, including MSCs, are able to induce obvious contraction of the collagen lattice (Fig. 6a). However, the four groups of differentiated cells and native VSMCs exhibited higher extent of collagen lattices contraction compared to MSCs (Fig. 6b). It is worth noting that the cells cocultured with fibroblasts reduced the gel size by $> 80\%$, similar to natural VSMCs. These functional testing results suggested that decellularized vessel ECM and fibroblasts are able to direct the differentiation of MSCs into functional VSMCs, which was supported by the high expression of VSMCs marker genes and proteins found in the cells harvested from the ECM and fibroblast coculture groups (Fig. 3 and Fig. 4).

4. Discussion

The limited source of VSMCs is one of the biggest obstacles to the development of artificial vessel grafts in vascular tissue engineering [5]. To address this challenge, establishing a new strategy for obtaining functional VSMCs is critical to blood vessels constitution. In this study, we assessed the effect of decellularized ECM and fibroblasts-coculture, GFC, and their combination on the MSCs differentiation toward VSMCs, an alternative approach to obtaining vascular cells. It is well documented that a combination of multiple growth factors exerted synergistic effect on the stem cell differentiation [10,20], therefore, in this study, a GFC of TGF β 1, PDGF-BB, and BMP4 were chosen as control experiment for inducing the differentiation of MSCs into VSMC-like cells. Our results indicated that both natural ECM and fibroblasts-coculture were able to stimulate the differentiation of MSCs toward VSMCs phenotype by upregulating the expression of VSMCs-specific markers (α -actin, calponin, smoothelin, SM-22 α , and MHC) and enhanced contractile functions. This study advanced our knowledge of how the microenvironmental factors provided by decellularized ECM or fibroblasts-coculture contribute to vascular tissue formation.

Natural ECM scaffolds are widely used to support cell adhesion, invasion, and migration in tissue engineering and regenerative medicine [24,31]. Collagen and fibronectin are the predominant components of vascular ECM [2,32], major ligand proteins for cell adhesion and growth. In addition to providing a suitable substrate for cell attachment in the vessel wall, a plethora of chemical signals existing in the ECM favor initiating cellular differentiation [33,34]. Our findings coincide with a recent report [35], where Shi et al. elucidated that cell culture substrates could dominate cell function and differentiation capacity. A positive correlation between growth factor activation and substrate stiffness might provide a reasonable explanation for the regulatory mechanism [17,36,37], by which vascular ECM directs MSCs differentiation toward VSMCs.

Cell-cell interaction is another modulatory process leading to vascular formation, which is distinct from cell-matrix interaction [33]. Endothelial cells in the tunica intima, VSMCs in the media, and fibroblasts in the adventitia are three main cell types present in the blood vessel wall [1]. Liu et al. revealed that endothelial cells could facilitate the proliferation and differentiation of VSMCs through an indirect coculture system [38]. However, the crosstalk between VSMCs and fibroblasts remains unclear. In this study, therefore, we hypothesized that indirect fibroblasts-coculture might be able to provide a positive effect on the differentiation of MSCs into VSMCs. Our results demonstrated that fibroblasts-coculture system successfully guided the MSCs differentiation toward VSMCs, and interestingly, its inductive capability was even stronger than GFC, demonstrated by higher expression of myogenic markers (Fig. 4) and enhanced contractile activity (Fig. 5 and Fig. 6). This finding is similar to a recent report that showed rat MSCs could differentiate into smooth muscle-like cells when cocultured with myofibroblasts to simulate vascular injury [38]. These observations may be attributed to cell-cell interactions elicited through paracrine factors released by fibroblasts [39], but the detailed underlying mechanism still needs to be further investigated. Lee et al. also reported that baboon smooth muscle cells cocultured with fibroblasts on the adventitial surface of the tubular constructs might increase collagen production and ECM organization, thereby augmenting mechanical properties of the constructed grafts [40]. Taken together, these findings did not only underscore the importance of adventitial fibroblasts on the domination of MSC fate, but also implicated the necessity of incorporating fibroblasts into engineered vascular tissues.

5. Conclusions

Our results demonstrated the strong capacity of native vascular ECM and adventitia fibroblasts-coculture in facilitating the differentiation of MSCs toward VSMC-like cells. The combined 3D coculture system provides an alternative approach to constructing artificial vessel graft for vascular tissue engineering and regeneration by integrating on-site differentiated functional VSMC-like cells into decellularized swine vascular scaffolds.

Supplementary Material

Refer to Web version on PubMed Central for supplementary material.

Acknowledgements

The authors would like to acknowledge Dr. Kevin Francis (Sanford Research Center, Sioux Falls) for providing fibroblasts, Mrs. Barb Haberer (Alumend, Sioux Falls) for providing porcine carotid arteries, Claire Evans (Imaging Core and Molecular Pathology Core, Sanford Research Center, Sioux Falls) for the assistance with histological experiments, and Dr. Erin B. Harmon for assistant with the microscopy. This work was supported, in part, by American Heart Association 15SDG25420001 (to Z. H.) and South Dakota Board of Regents UP1600205 (to Z. H.). This material is based upon work supported by the National Science Foundation/EPSCoR Cooperative Agreement #IIA-1355423 and by the State of South Dakota. Any opinions, findings, and conclusions or recommendations expressed in this material are those of the authors and do not necessarily reflect the views of the National Science Foundation.

References

- [1]. Wang YY, Hu J, Jiao J, Liu ZN, Zhou Z, Zhao C, Chang LJ, Chen YE, Ma PX, Yang B, Engineering vascular tissue with functional smooth muscle cells derived from human iPS cells and nanofibrous scaffolds, *Biomaterials* 35 (2014) 8960–8969. [PubMed: 25085858]
- [2]. Parvizi M, Bolhuis-Versteeg LAM, Poot AA, Harmsen MC, Efficient generation of smooth muscle cells from adipose-derived stromal cells by 3D mechanical stimulation can substitute the use of growth factors in vascular tissue engineering, *Biotechnol. J* 11 (2016) 932–944. [PubMed: 26989865]
- [3]. Krenning G, Moonen J, van Luyn MJA, Harmsen MC, Vascular smooth muscle cells for use in vascular tissue engineering obtained by endothelial-to-mesenchymal transdifferentiation (EnMT) on collagen matrices, *Biomaterials* 29 (2008) 3703–3711. [PubMed: 18556062]
- [4]. Serbo JV, Gerecht S, Vascular tissue engineering: biodegradable scaffold platforms to promote angiogenesis, *Stem Cell Res Ther* 4 (2013).
- [5]. Bajpai VK, Andreadis ST, Stem cell sources for vascular tissue engineering and regeneration, *Tissue Eng. Part B Rev* 18 (2012) 405–425. [PubMed: 22571595]
- [6]. Choi K, Kennedy M, Kazarov A, Papadimitriou JC, Keller G, A common precursor for hematopoietic and endothelial cells, *Development* 125 (1998) 725–732. [PubMed: 9435292]
- [7]. Hirashima M, Kataoka H, Nishikawa S, Matsuyoshi N, Nishikawa SI, Maturation of embryonic stem cells into endothelial cells in an in vitro model of vasculogenesis, *Blood* 93 (1999) 1253–1263. [PubMed: 9949168]
- [8]. Hirashima M, Ogawa M, Nishikawa S, Matsumura K, Kawasaki K, Shibuya M, Nishikawa SI, A chemically defined culture of VEGFR2(+) cells derived from embryonic stem cells reveals the role of VEGFR1 in tuning the threshold for VEGF in developing endothelial cells, *Blood* 101 (2003) 2261–2267. [PubMed: 12406893]
- [9]. Owens GK, Kumar MS, Wamhoff BR, Molecular regulation of vascular smooth muscle cell differentiation in development and disease, *Physiol. Rev* 84 (2004) 767–801. [PubMed: 15269336]
- [10]. Wang C, Yin S, Cen L, Liu QH, Liu W, Cao YL, Cui L, Differentiation of adipose-derived stem cells into contractile smooth muscle cells induced by transforming growth factor-beta 1 and bone morphogenetic Protein-4, *Tissue Eng. A* 16 (2010) 1201–1213.
- [11]. Zhang WJ, Liu W, Cui L, Cao YL, Tissue engineering of blood vessel, *J. Cell. Mol. Med* 11 (2007) 945–957. [PubMed: 17979876]
- [12]. El-Mounayri O, Mihic A, Shikatani EA, Gagliardi M, Steinbach SK, Dubois N, DaCosta R, Li RK, Keller G, Husain M, Serum-free differentiation of functional human coronary-like vascular smooth muscle cells from embryonic stem cells, *Cardiovasc. Res* 98 (2013) 125–135. [PubMed: 23213107]
- [13]. Parmar N, Ahmadi R, Day RM, A novel method for differentiation of human mesenchymal stem cells into smooth muscle-like cells on clinically deliverable thermally induced phase separation microspheres, *Tissue Eng. Part C Methods* 21 (2015) 404–412. [PubMed: 25205072]
- [14]. Jack GS, Zhang R, Lee M, Xu YH, Wu BM, Rodriguez LV, Urinary bladder smooth muscle engineered from adipose stem cells and a three dimensional synthetic composite, *Biomaterials* 30 (2009) 3259–3270. [PubMed: 19345408]

- [15]. Kinner B, Zaleskas JM, Spector M, Regulation of smooth muscle actin expression and contraction in adult human mesenchymal stem cells, *Exp. Cell Res* 278 (2002) 72–83. [PubMed: 12126959]
- [16]. Wang DJ, Park JS, Chu JSF, Krakowski A, Luo KX, Chen DJ, Li S, Proteomic profiling of bone marrow mesenchymal stem cells upon transforming growth factor beta 1 stimulation, *J. Biol. Chem* 279 (2004) 43725–43734. [PubMed: 15302865]
- [17]. Floren M, Bonani W, Dharmarajan A, Motta A, Migliaresi C, Tan W, Human mesenchymal stem cells cultured on silk hydrogels with variable stiffness and growth factor differentiate into mature smooth muscle cell phenotype, *Acta Biomater.* 31 (2016) 156–166. [PubMed: 26621695]
- [18]. Dash BC, Levi K, Schwan J, Luo J, Bartulos O, Wu HW, Qiu CH, Yi T, Ren YM, Campbell S, Rolle MW, Qyang YB, Tissue-engineered vascular rings from human iPSC-derived smooth muscle cells, *Stem Cell Rep.* 7 (2016) 11–20.
- [19]. Yan PK, Xia CL, Duan CW, Li SH, Mei ZR, Biological characteristics of foam cell formation in smooth muscle cells derived from bone marrow stem cells, *Int. J. Biol. Sci* 7 (2011) 937–946. [PubMed: 21850203]
- [20]. Elcin AE, Parmaksiz M, Dogan A, Seker S, Durkut S, Dalva K, Elcin YM, Differential gene expression profiling of human adipose stem cells differentiating into smooth muscle-like cells by TGF beta 1/BMP4, *Exp. Cell Res* 352 (2017) 207–217. [PubMed: 28185836]
- [21]. Bouten CVC, Dankers PYW, Driessen-Mol A, Pedron S, Brizard AMA, Baaijens FPT, Substrates for cardiovascular tissue engineering, *Adv. Drug Deliv. Rev* 63 (2011) 221–241. [PubMed: 21277921]
- [22]. Stegemann JP, Kaszuba SN, Rowe SL, Review: advances in vascular tissue engineering using protein-based biomaterials, *Tissue Eng.* 13 (2007) 2601–2613. [PubMed: 17961004]
- [23]. Zhao YL, Zhang ZG, Wang JL, Yin P, Wang Y, Yin ZY, Zhou JY, Xu G, Liu Y, Deng ZG, Zhen MC, Cui WG, Liu ZC, Preparation of decellularized and cross-linked artery patch for vascular tissue-engineering application, *J. Mater. Sci. Mater. Med* 22 (2011) 1407–1417. [PubMed: 21528356]
- [24]. Mancuso L, Gualerzi A, Boschetti F, Loy F, Cao G, Decellularized ovine arteries as small-diameter vascular grafts, *Biomed. Mater* 9 (2014).
- [25]. Discher DE, Mooney DJ, Zandstra PW, Growth factors, matrices, and forces combine and control stem cells, *Science* 324 (2009) 1673–1677. [PubMed: 19556500]
- [26]. Kuraitis D, Giordano C, Ruel M, Musaro A, Suuronen EJ, Exploiting extracellular matrix-stem cell interactions: a review of natural materials for therapeutic muscle regeneration, *Biomaterials* 33 (2012) 428–443. [PubMed: 22014942]
- [27]. Wang G, Jacquet L, Karamariti E, Xu QB, Origin and differentiation of vascular smooth muscle cells, *J. Physiol. Lond* 593 (2015) 3013–3030. [PubMed: 25952975]
- [28]. Katsimpoulas M, Morticelli L, Michalopoulos E, Gontika I, Stavropoulos-Giokas C, Kostakis A, Haverich A, Korossis S, Investigation of the biomechanical integrity of decellularized rat abdominal aorta, *Transplant. Proc* 47 (2015) 1228–1233. [PubMed: 26036560]
- [29]. Li N, Wang DD, Sui ZG, Qi XY, Ji LY, Wang XL, Yang L, Development of an improved three-dimensional in vitro intestinal mucosa model for drug absorption evaluation, *Tissue Eng. Part C Methods* 19 (2013) 708–719. [PubMed: 23350801]
- [30]. Luo JS, Qin LF, Kural MH, Schwan J, Li X, Bartulos O, Cong XQ, Ren YM, Gui LQ, Li GX, Ellis MW, Li PN, Kotton DN, Dardik A, Pober JS, Tellides G, Rolle M, Campbell S, Hawley RJ, Sachs DH, Niklason LE, Qyang YB, Vascular smooth muscle cells derived from inbred swine induced pluripotent stem cells for vascular tissue engineering, *Biomaterials* 147 (2017) 116–132. [PubMed: 28942128]
- [31]. Bergmeister H, Strobl M, Grasl C, Liska R, Schima H, Tissue engineering of vascular grafts, *Eur. Surg* 45 (2013) 187–193.
- [32]. Eble JA, Niland S, The extracellular matrix of blood vessels, *Curr. Pharm. Des* 15 (2009) 1385–1400. [PubMed: 19355976]
- [33]. Martino MM, Briquez PS, Guc E, Tortelli F, Kilarski WW, Metzger S, Rice JJ, Kuhn GA, Muller R, Swartz MA, Hubbell JA, Growth factors engineered for super-affinity to the extracellular matrix enhance tissue healing, *Science* 343 (2014) 885–888. [PubMed: 24558160]

- [34]. Dew L, MacNeil S, Chong CK, Vascularization strategies for tissue engineers, *Regen. Med* 10 (2015) 211–224. [PubMed: 25835483]
- [35]. Shi ZL, Neoh KG, Kang ET, Poh CK, Wang W, Enhanced endothelial differentiation of adipose-derived stem cells by substrate nanotopography, *J. Tissue Eng. Regen. Med* 8 (2014) 50–58. [PubMed: 22628362]
- [36]. Wingate K, Floren M, Tan Y, Tseng PON, Tan W, Synergism of matrix stiffness and vascular endothelial growth factor on mesenchymal stem cells for vascular endothelial regeneration, *Tissue Eng. A* 20 (2014) 2503–2512.
- [37]. Wipff PJ, Rifkin DB, Meister JJ, Hinz B, Myofibroblast contraction activates latent TGF-beta 1 from the extracellular matrix, *J. Cell Biol* 179 (2007) 1311–1323. [PubMed: 18086923]
- [38]. Liu YX, Rayatpisheh S, Chew SY, Chan-Park MB, Impact of endothelial cells on 3D cultured smooth muscle cells in a biomimetic hydrogel, *ACS Appl. Mater. Interfaces* 4 (2012) 1378–1387. [PubMed: 22296557]
- [39]. Wendan Y, Changzhu J, Xuhong S, Hongjing C, Hong S, Dongxia Y, Fang X, BMSCs interactions with adventitial fibroblasts display smooth muscle cell lineage potential in differentiation and migration that contributes to neointimal formation, *Stem Cells Int* (2016), 10.1155/2016/3196071(2016).
- [40]. Lee KW, Stolz DB, Wang YD, Substantial expression of mature elastin in arterial constructs, *Proc. Natl. Acad. Sci. U. S. A* 108 (2011) 2705–2710. [PubMed: 21282618]

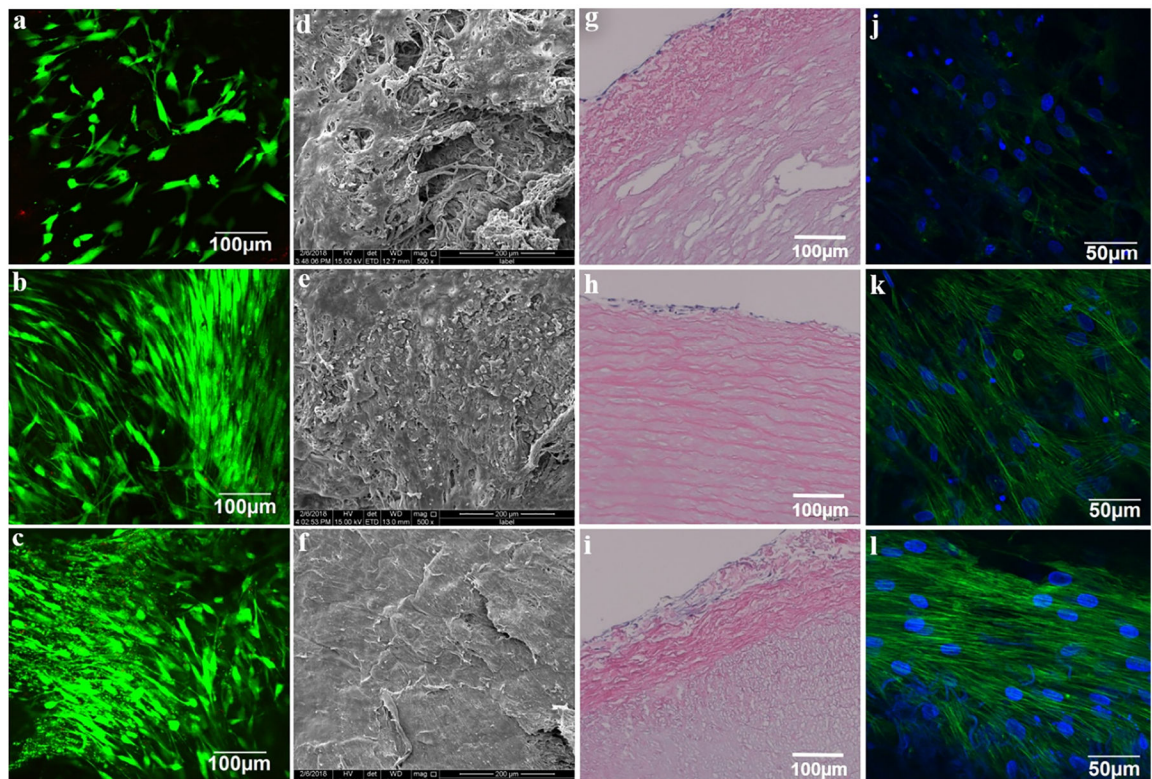


Fig. 1.

Viability and morphological characteristics of the cells in a combined 3D coculture model. Live-dead staining for MSCs seeded in decellularized ECM scaffold, on (a) day 1, (b) day 7 and (c) day 14. SEM images showed the representative morphology of adventitial surface of the vessel ECM scaffold post MSCs-seeding, on (d) day 1, (e) day 7 and (f) day 14. HE staining for vessel ECM scaffold post MSCs-seeding, on (g) day 1, (h) day 7 and (i) day 14 showed progressive cell migration into the decellularized ECM scaffold. F-actin staining using phalloidin for MSCs seeded on the adventitial side of ECM scaffold, on (j) day 1, (k) day 7 and (l) day 14 showed increasing fluorescence intensity of actin stress fibers in cells cultured on the ECM scaffold.

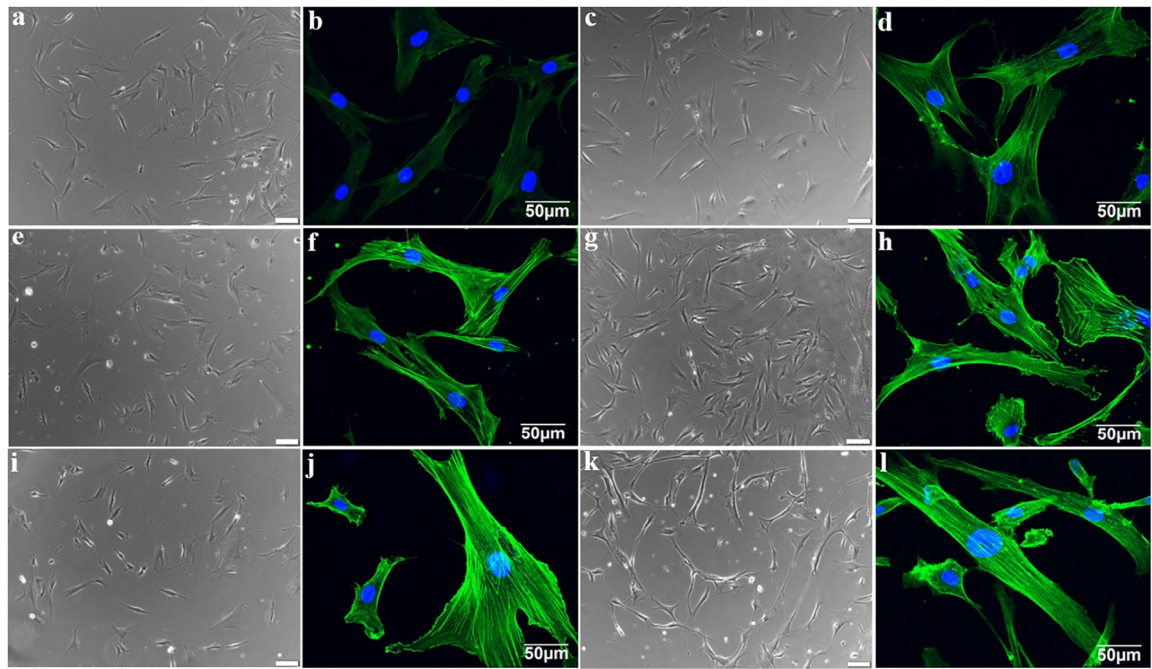


Fig. 2.

Respective and combinational effects of ECM, fibroblasts and growth factors cocktail (GFC) on the morphology of MSCs. (a) Phase contrast and (b) confocal microscopy images of primary MSCs. (c) Phase contrast and (d) confocal microscopy images of MSCs after 14-day indirect cocultured with fibroblasts. (e) Phase contrast and (f) confocal microscopy images of MSCs after 14-day cultured with GFC. (g) Phase contrast and (h) confocal microscopy images of MSCs after 14-day cultured on the decellularized ECM scaffold. (i) Phase contrast and (j) confocal microscopy images of MSCs after 14-day cultured in the combined 3D coculture model. (k) Phase contrast and (l) confocal microscopy images of VSMCs. Similar to GFC, both decellularized ECM scaffold and indirect coculturing with fibroblasts have the capability to induce the differentiation of MSCs toward VSMCs.

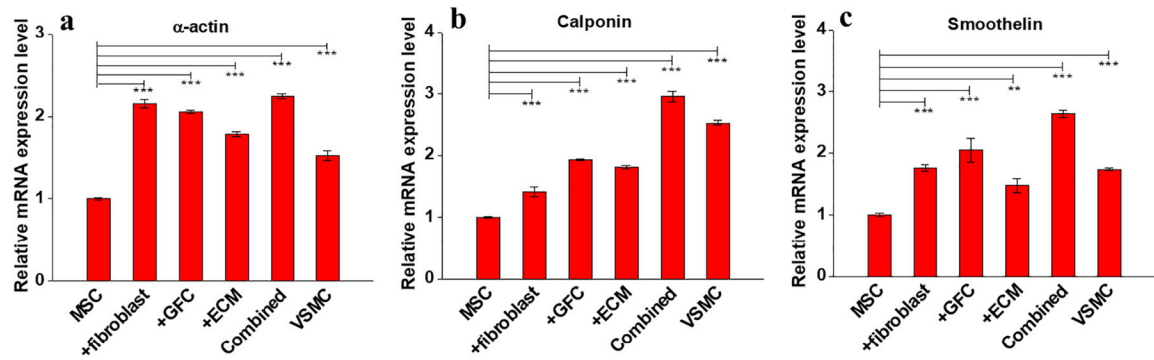


Fig. 3.

Real time RT-PCR analysis for the expression of VSMCs marker genes in MSCs under different culture conditions for 14 days. (a) Relative mRNA expression of α -actin. (b) Relative mRNA expression of calponin. (c) Relative mRNA expression of smoothelin. Similar to GFC, both decellularized ECM scaffold and indirect fibroblasts-coculture significantly upregulated the expression of VSMC-specific marker genes. Data are expressed as mean \pm SD ($n = 3$). ** $P < 0.01$, *** $P < 0.001$.

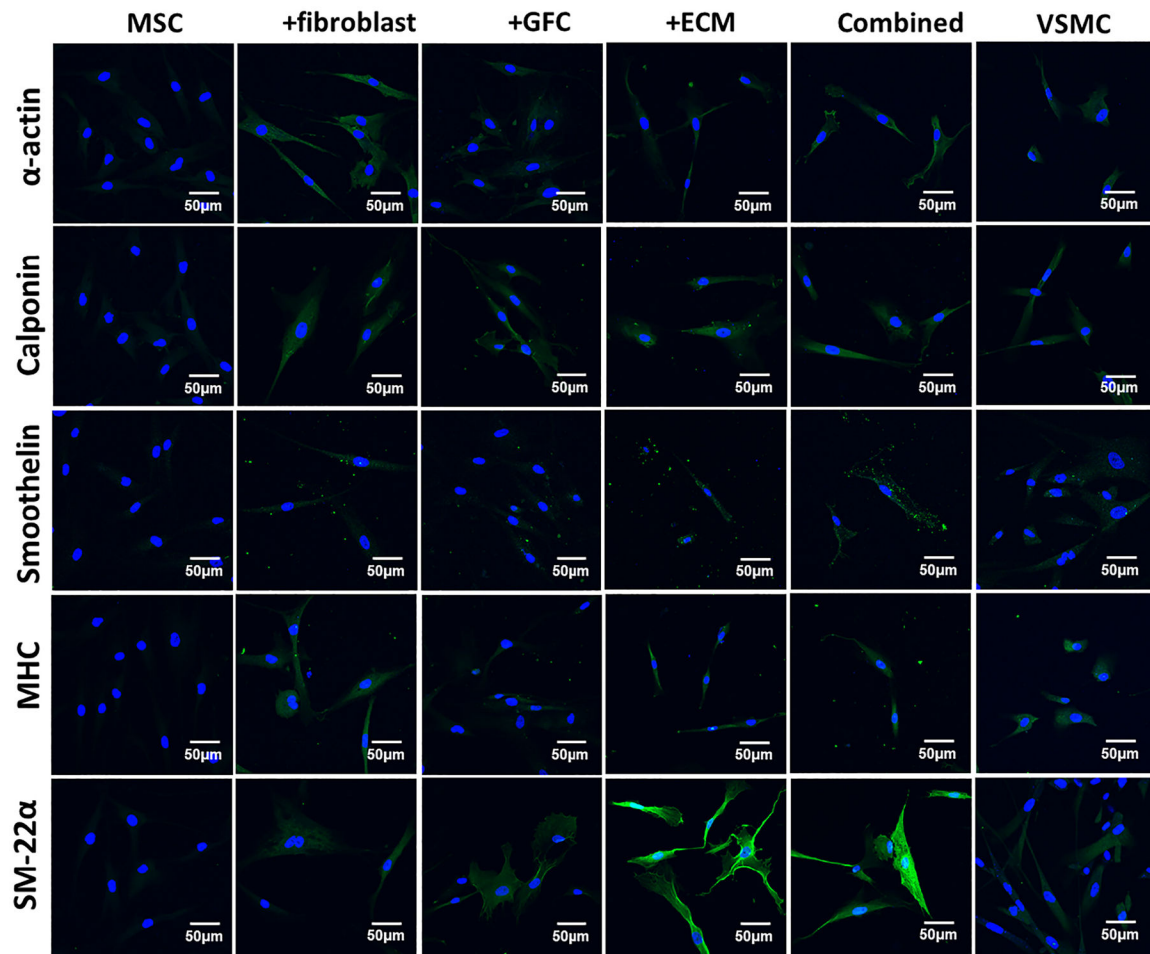


Fig. 4. Immunofluorescence staining for VSMC-specific proteins including α -actin, calponin, smoothelin, myosin heavy chain (MHC), and smooth muscle protein 22 α (SM-22 α) in MSCs under different culture conditions for 14 days. Cell nuclei were counterstained with Hoechst 33342. Compared to MSCs, the fluorescence intensity (expression) of marker proteins in the differentiated cells induced by ECM scaffold, fibroblasts-coculture, GFC, or combined 3D coculture model were significantly increased. Fibroblasts and ECM appeared to be stronger regulators than GFC on the expression of α -actin, calponin, smoothelin, and MHC. In addition, the cells under ECM and combined 3D coculture condition demonstrated much higher fluorescence intensity for SM-22 α than other experimental groups. The images represent at least three independent experiments.

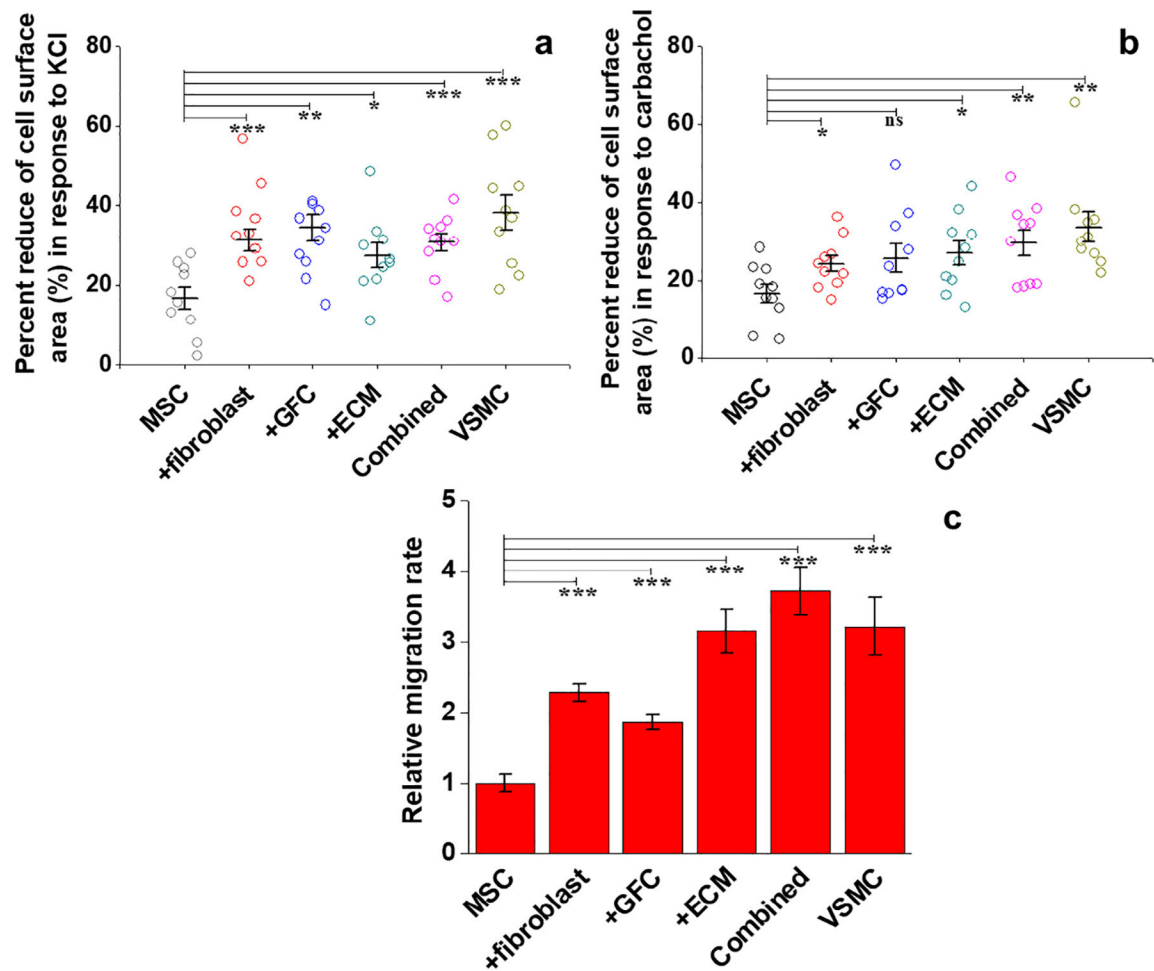


Fig. 5. Functional analysis of VSMCs-like cells derived from MSCs under different experimental conditions. (a) Percentage area decrease for each cell population under stimulation with KCl ($n = 10$). (b) Percentage area decrease for each cell group under stimulation with carbachol ($n = 10$). (c) Relative cell migration rate toward PDGF-BB gradient for each cell group. All cell populations differentiated under four different conditions exhibited much stronger VSMC-specific functions than primary MSCs, indicating the potential capability of ECM and fibroblasts in promoting the differentiation of MSCs toward normal functional VSMCs. Data are expressed as mean \pm SD ($n = 3$). ns $P > 0.05$, * $P < 0.05$, ** $P < 0.01$, *** $P < 0.001$.

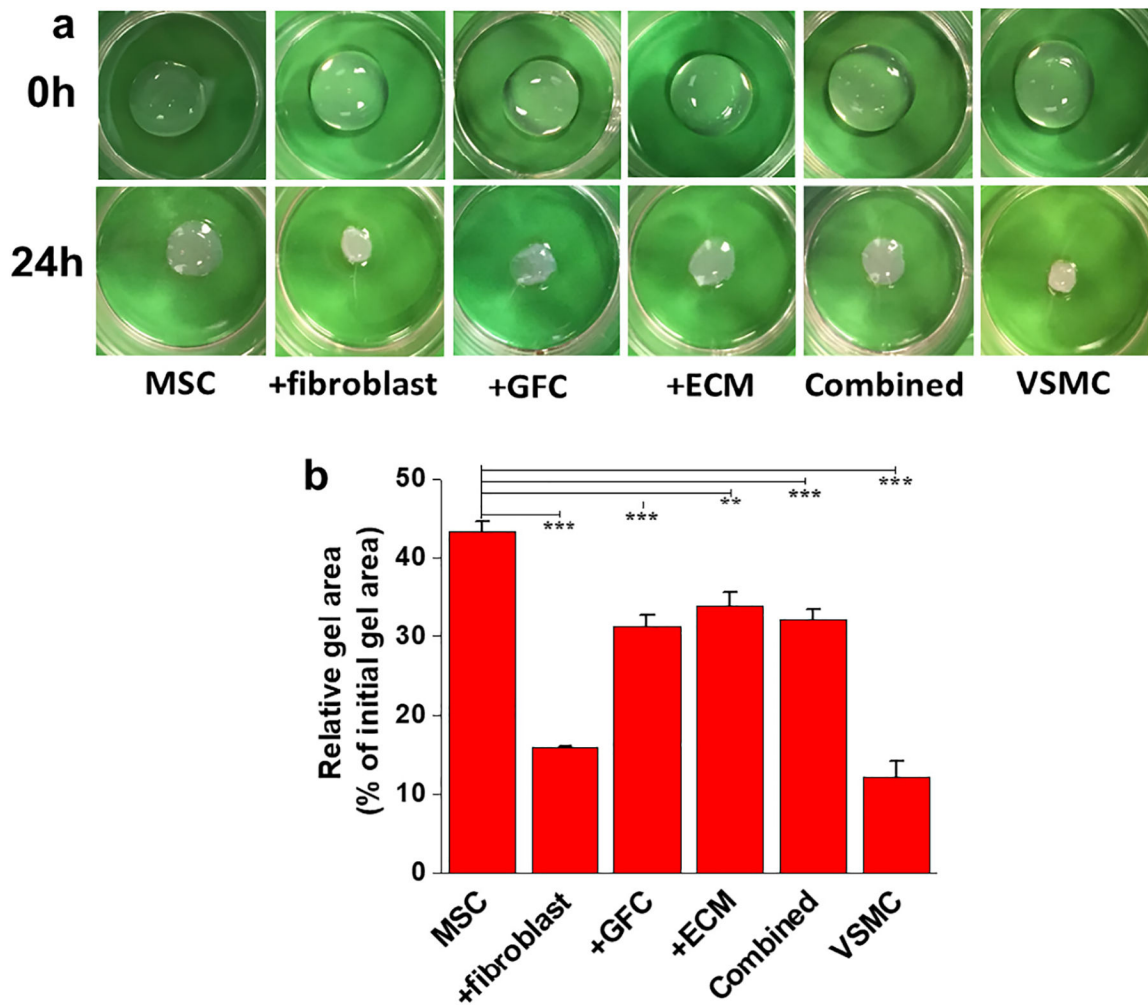


Fig. 6. Contraction of collagen lattice by resident VSMCs-like cells derived from MSCs under different experimental conditions. (a) Representative images showing the contraction of collagen gel by resident six different groups of cells. (b) Quantification of collagen lattice contraction by different resident cell groups after 24 h. The collagen lattices populated by the cells differentiated under all four conditions exhibited higher contractility compared to the MSCs. Especially, the cells after coculture with fibroblasts showed the highest contractility similar to natural VSMCs. Data are expressed as mean \pm SD ($n = 3$). ** $P < 0.01$, *** $P < 0.001$.